doi:10.1017/S1431927621002312
Microsc. Microanal. 27 (Suppl 1), 2021
© Microscopy Society of America 2021

Fast Method for Estimating Stain Density in Electron Microscopy of Conventionally Prepared Biological Specimens

Richard Leapman[1], Andrea Fera[2], Guofeng Zhang[1] and Qianping He[1]

[1]NIBIB, National Institutes of Health, Bethesda, Maryland, United States, [2]Reveal Global Consulting, United States

A variety of 3D electron microscopy techniques provides biologists with nanoscale ultrastructure that underlies the mechanisms for a wide range of important cellular processes. These methods include serial block-face scanning electron microscopy (SBF-SEM) and focused ion beam scanning electron microscopy (FIB-SEM) (1-3). In both these approaches, embedded blocks of cells or tissues are imaged in a scanning electron microscope using the backscattered electron signal generated by scattering of electrons from heavy-atom stain incorporated into the biological specimens after fixation and prior to embedding. Optimization of sample preparation is crucial for obtaining the best results from SBF-SEM and FIB-SEM. Too little stain produces images with poor signal-to-noise ratio, which reduces visibility of ultrastructure, and can also result in deleterious specimen charging, yet too much stain can mask subtle ultrastructural features. In the acquisition of 3D images of ultrastructure using SBF-SEM, the fluence of incident electrons is limited to approximately 20 electrons/nm2 due to shrinkage of the block caused by radiation damage. If higher doses are used, the specimen block will not cut evenly at smaller cutting increments (4).

Here, we demonstrate a straightforward technique for determining stain density in embedded biological specimens using conventional bright-field TEM imaging of sections that are cut from the same blocks that are subsequently analyzed by SBF-SEM or FIB-SEM. The robustness of the method is demonstrated for sections cut at a thickness from 100 nm to 750 nm, and the same stain density is obtained regardless of the specimen thickness, or whether there is mass loss caused by electron irradiation, and the measurements and analysis can be performed in a few minutes (5)

Based on the observed lack of contrast in unstained embedded biological structures, it is assumed here that the unstained biological material does not attenuate the primary electron beam due to elastic scattering more than the surrounding clear (unstained) resin. This is expected since the light atoms in the resin have approximately the same mass as the atoms in the biological tissue or cells. For a plastic section of thickness t containing embedded cells or tissue and regions of pure embedding medium, we can write:

$$\Sigma h\, n_h\, \sigma_h = (1/t)\, \ln(I_{resin}/I_{cell})$$

where n_h is the number of heavy atoms of stain of type h per unit volume, σ_h is the elastic scattering cross section of heavy atom h, I_{cell} is the transmitted fluence through the cell, and I_{cell} is the transmitted fluence through the pure resin. The total number of heavy atoms of stain per unit volume is given by:

$$n_H = [t\, \Sigma_h\, f_h\, \sigma_h]^{-1} \ln(I_{resin}/I_{cell})$$

where $f_h = n_h/n_H$.

https://doi.org/10.1017/S1431927621002312 Published online by Cambridge University Press

Accurate solid-angle differential scattering cross sections, as a function of scattering angle θ, are now available as a Standard Reference Database SRD 64 from the National Institute of Standards and Technology (6,7). We have used this database to integrate the differential cross sections over scattering angles subtended by a 10-mrad semi-angle objective aperture in a 300 keV TEM for atoms of osmium, lead, and uranium.

The use of this method to determine the concentrations of stain in a block of mouse brain prepared for SBF-SEM is illustrated in Figure 1, which shows bright-field images of sectioned mouse brain of nominal thicknesses of 0.25 µm, 0.5 µm, 0.75 µm, and 1.0 µm, recorded at a beam energy of 300 keV. A plot of $ln(I_{resin}/I_{cell})$ as a function of specimen thickness t in Figure 2 shows a straight line through the origin with a slope of $1.44 \pm 0.06 \times 10^{-3}$ nm^{-1}. After dividing by the elastic cross section of 0.00085 nm^2 is obtained for the Pb cross section for semi-angle 10 mrad, we obtain a stain density of 1.70 ± 0.07 heavy atoms per nm^3. This specimen was prepared using the UCSD NCMIR protocol (8).

We have tested the method on three specimens with different levels of staining and the results appear to be consistent; blocks prepared with the UCSD NCMIR protocols have the highest stain concentration, and samples prepared for thick-section STEM tomography have a stain concentration that is a factor of between 3–5 times smaller.

Since the number of light atoms from the resin and biological material do not appear in the expression for the stain concentration, the number of heavy atoms per unit volume is computed directly. The inverse product of the thickness and the scattering cross section in this expression has units of nm^{-3}, so that the measurement needed to determine the stain concentration is a dimensionless quantity that is independent of the light atoms. This makes the method very robust with respect to mass loss during bright-field imaging, or contamination deposited on the section while being imaged in the column of the TEM.

In our experience, considerable time is wasted by imaging specimens in which the stain concentration is not well suited to the imaging technique, and it is often not possible to assess the stain concentration by inspection of the specimen in the optical microscope, since even at low concentration osmium causes black staining of the block, whereas lead and uranium are not easily visible. The method described here can be applied very quickly, simply by recording a few bright field images. Moreover, it is not necessary to use a 300-keV TEM, and measurements can be made just as easily at beam energies of 100 or 120 keV (9).

https://doi.org/10.1017/S1431927621002312 Published online by Cambridge University Press

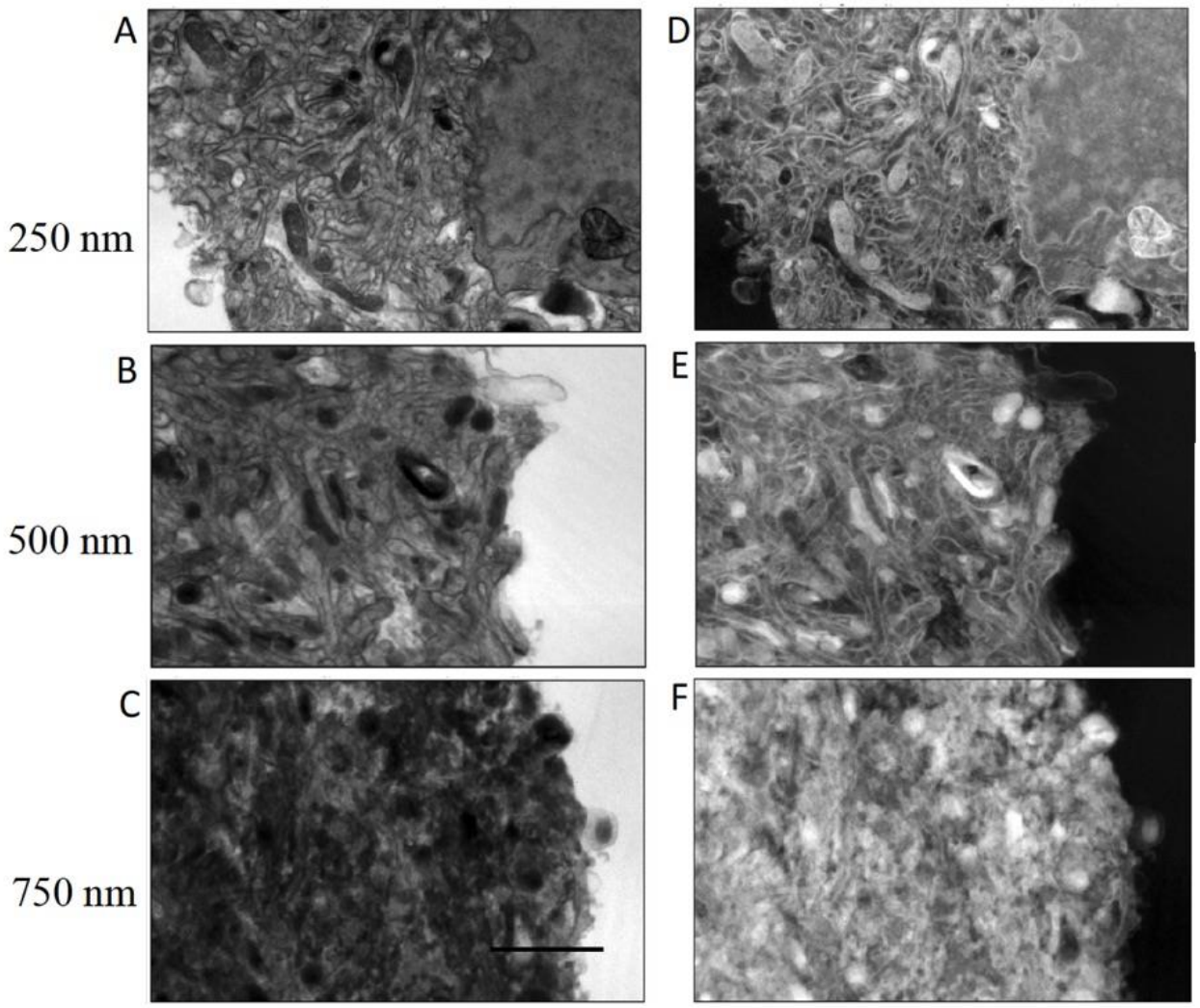

Figure 1. Analysis of bright-field TEM images *I(x,y)* from sections of mouse brain in specimens of different thicknesses: (A) 250 nm; (B) 500 nm; (C) 750 nm. Corresponding computed images of $\ln[I_{resin}/I(x,y)]$ are shown in (D) for the 250-nm section; (E) for the 500-nm section; and (F) for the 750-nm section. Values for I_{resin} were obtained by averaging the intensity of the pixels contained in regions of clear embedding resin surrounding the cells. Scale bar = 2 μm.

https://doi.org/10.1017/S1431927621002312 Published online by Cambridge University Press

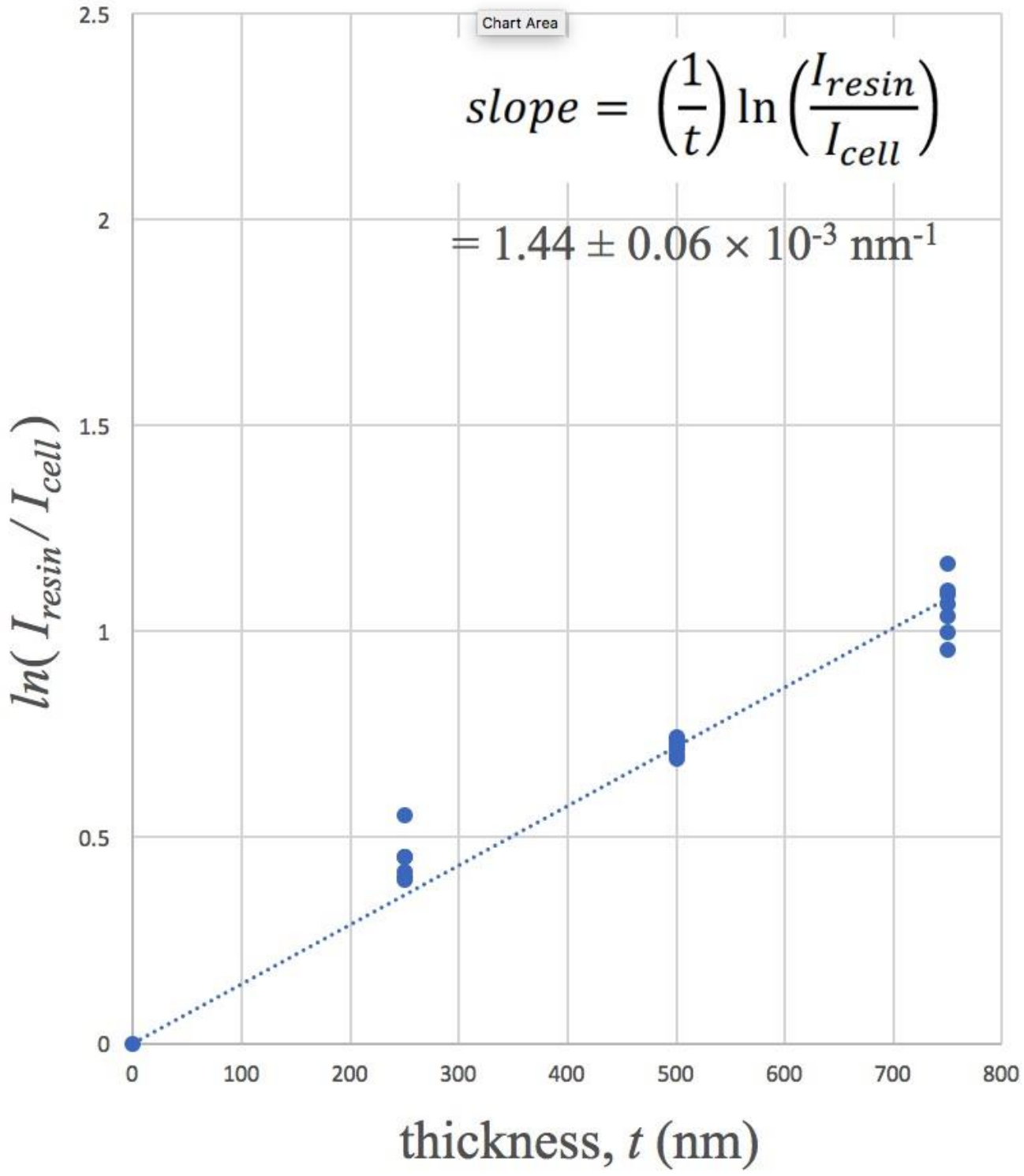

Figure 2. Plot of the mean value of ln[$I_{resin}/I(x,y)$] versus specimen thickness t for a sample of mouse brain sample. The points are fit by a straight line through the origin.

https://doi.org/10.1017/S1431927621002312 Published online by Cambridge University Press

References

1. W. Denk, H. Horstmann, PLoS Biol. 2, e329 (2004).

2. L.H.P. Hekking et al., J. Microsc. 235, 336–347 (2009).

3. K. Narayan, S. Subramaniam, Nat. Methods. 12(11), 1021-1031 (2015).

4. C. Kizilyaprak et al., J. Struct. Biol. 189, 135-146, (2015).

5. A. Fera et al., J. Microsc. 277(2), 71-78 (2020).

6. F. Salvat, A. Jablonski, C.J. Powell, National Institute of Standards and Technology, USA, NIST electron elastic-scattering cross-section database, SRD 64 (2002)

7. F. Salvat, A. Jablonski, C.J. Powell, Comput. Phys. Commun. 165, 157-190 (2005).

8. T.J. Deerinck et al., NCMIR Methods for 3D EM (2010).

9. This work was supported by the Intramural Research Program of NIBIB, NIH.

https://doi.org/10.1017/S1431927621002312 Published online by Cambridge University Press